J Mater Sci (2016) 51:5791–5801

A new insight to the effect of calcium concentration on gelation process and physical properties of alginate films

Jiwei Li[1], Yadong Wu[1], Jinmei He[1,*], and Yudong Huang[1]

[1] *School of Chemical Engineering and Technology, Harbin Institute of Technology, Harbin 150001, China*

Received: 19 January 2016
Accepted: 3 March 2016
Published online: 8 March 2016

ABSTRACT

A series of alginate films were prepared using constant alginate content (2 % w/v) with various calcium chloride ($CaCl_2$) concentrations in the crosslinking solution (0.375–6 % w/v). Then, the initial investigation of how the $CaCl_2$ concentration affected the gelation process and physical properties of alginate films was established. A combination of Fourier transform infrared spectroscopy, swelling test, inductively coupled plasma optical emission spectrometer, and energy-dispersive spectroscopy analysis showed that the gelation process of alginate films evolved with the increase of $CaCl_2$ concentration, which resulted in different crosslinking density and entanglement of alginate molecular chains. Moreover, the increase of $CaCl_2$ concentration improved the visual appearance, surface homogeneity, and tensile strength, while the elongation at break and swelling capacity of the film were decreased monotonously. As a compromise between film strength and flexibility, performing effective absorption capability as well as the product appearance, the concentration of 1.5 % w/v $CaCl_2$ in the crosslinking step was recommended. These various physical properties of obtained alginate films could be attributed to the shaped crosslinking density and molecular entanglement characteristics during crosslinking.

Introduction

Sodium alginate (SA) is a linear water-soluble polysaccharide consisting of monomeric units of 1–4 linked α-D-mannuronate (M) and β-L-guluronate (G) at different proportions in the chain [1–3]. The unique chemical structure of SA and its biocompatibility, non-toxicity, low cost, and functional gelation have made it an important polymer in biomedical applications including wound dressings [4, 5], drug delivery [6–8], and tissue engineering [9, 10]. For several applications, alginate is used as a film-forming material as it has the ability for film formation upon casting or solvent evaporation.

Alginate and polyvalent cations (such as Ca^{2+}, Ba^{2+}, Zn^{2+}, and Cu^{2+}) could readily crosslink and

Address correspondence to E-mail: hejinmeihit@163.com; hejinmei@hit.edu.cn

DOI 10.1007/s10853-016-9880-0

form the "egg-box" structure through ionic linkage between polyvalent cations and an ionic G–G-rich sequences along the polysaccharide backbone [11–13]. To develop and tailor alginate formulations for biomedical applications, the knowledge about the gelling mechanism of alginate materials is of great importance. The earliest regenerated alginate fibers were produced in the 1930s [14, 15]. Since then, considerable amounts of research effort have been expended to understand the relationships between coagulation conditions, properties and morphology of alginate fibers [16, 17]. For example, Cuadros et al. investigate the effect of concentration of $CaCl_2$ on the mechanical properties of calcium alginate fibers and found that maximum tensile stress was obtained for a $CaCl_2$ around 1.4 % which exceeded several times the stoichiometric requirements of the carboxylate groups of the polymer [18]. In addition, the effects of calcium ion concentration on the functional properties of alginate materials have also been reported. For instance, Akin Evingür et al. found that the coefficients for small molecule desorption from alginate beads increased up to 3 % (w/v) $CaCl_2$ concentration, and then decreased with a further increase of $CaCl_2$ content [19]. Recently, the solution phase interaction between the polysaccharide alginate and calcium at various $CaCl_2$ concentrations was reported by Xin et al. [20]. Although some previous studies have reported that varying $CaCl_2$ concentrations affected the physical properties of alginate fibers, to our knowledge, the interaction between Ca^{2+} and molecular chains of alginate films during the external gelation process has not been reported.

Therefore, the objective of this study is to investigate the influence of calcium concentration on gelation process of alginate films. In addition, the effects of calcium concentration on the visual appearance, thickness, surface homogeneity, swelling, and mechanical properties were systematically investigated.

Materials and methods

Materials

Sodium alginate (SA, pharmaceutical grade, low viscosity, M/G $\approx$ 6:4) was kindly provided by Qingdao Hyzlin Biology Development Co., Ltd (China).

Calcium chloride ($CaCl_2$) and ethanol were of analytical grade and purchased from commercial sources in Weihai, China.

Preparation of films

Preparation of sodium alginate films

Films were prepared by casting from aqueous solutions. An aqueous solution of sodium alginate was prepared by dissolving 2 g of sodium alginate powder in 100 ml distilled water to obtain a 2 % w/v alginate solution, using a magnetic stirring plate at 25 °C and 400 rpm for 6 h. All solutions were filtered through 0.45-μm membrane filter and kept for a few minutes under vacuum. After this treatment, solutions were cast onto petri dishes and allowed to dry in an oven at 35 °C for approximately 24 h. To control film thickness, volume of each film-forming solution poured onto a petri dish remained the same. The dried films were then removed from the petri dishes and stored in desiccators for at least 48 h before being used.

Preparation of crosslinked alginate films

Dry-cast gelation (DCG) and interfacial gelation (IFG) are two methods that have been employed to produce ionic gel films [21, 22]. Since DCG involves producing a dry film of sodium alginate before it is gelled, whereas the latter involves producing calcium alginate gel films in situ within the SA solution, DCG would produce denser and more integrated films than IFG [21]. Therefore, calcium alginate (Ca-SA) films were prepared by a modified dry-cast external gelation method reported in a previous study [23]. The crosslinking solution was prepared by dissolving $CaCl_2$ powder in ethanol/water (v/v = 20/80) solvent solutions. The concentrations of $CaCl_2$ in the crosslinking solution were 0.375, 0.75, 1.5, 3 and 6 % w/v, respectively. Each dried sodium alginate film (about 0.4 g) was immersed in 100 ml of crosslinking solution for 1 h. The crosslinked films were washed with deionized water thrice to remove any surface unbound cations before drying to constant weight at 25 °C. The films harvested were then stored in a desiccator for at least 48 h before use.

Infrared spectroscopy

In order to confirm the crosslinking reaction, Fourier Transform Infrared Spectroscopy (FTIR) measurements were performed by a Perkin-Elmer System 2000 spectrometer. The analysis was performed using an attenuated total reflectance (ATR) cell, in a range of 4000–600 cm^{-1}, at a 4 cm^{-1} resolution with 64 scans.

Scanning electron microscopy (SEM) and energy-dispersive spectroscopy (EDS) analysis

SEM observation and energy-dispersive spectroscopy (EDS) measurements were carried out by a SU8010 scanning electron microscope (Hitachi, Japan) equipped with an energy-dispersive spectroscopy detector. Cross sections were obtained by cracking the films in liquid nitrogen.

Swelling studies

To determine the SD, the excess crosslinking solution on the surface of film samples (2 × 2 cm) was removed with a filter paper and then their wet weights were immediately determined to calculate the SD by Eq. (1).

$$SD = \frac{(W_w - W_d)}{W_d} \times 100\,\%, \quad (1)$$

where W_w represents the wet weight of the films and W_d corresponds to the dry weight of SA films.

The swelling ratio (SR) of crosslinked films was determined by measuring the change in film weight during incubation in a distilled water solution at 25 °C and calculated as follows:

$$SR = \frac{(W_{wi} - W_d)}{W_d}, \quad (2)$$

where W_{wi} represents the wet weight of films in the i minute and W_d corresponds to the dry weight of the films.

Determination of the calcium content

The calcium content was determined by inductively coupled plasma optical emission spectrometer (ICP-OES) Optima 8300 (Perkin-Elmer, Massachusetts, USA). About 8 mg film samples were dissolved in 10 mL of a calcium ion chelator, EDTA (0.05 M) for 24 h to free the Ca^{2+} crosslinked within the alginate hydrogel, and then the solutions were analyzed. The EDTA solution was used as a blank measurement. All tests were performed in triplicate.

Determination of the thickness

The film thickness was measured using a micrometer (0.001 mm, SF 2000, Guanglu Co., Ltd) at 10 different positions of the film. For the wet films after crosslinking, the excess of water was removed with a filter paper and then the film thickness was measured. At least 10 replicates were run for each sample.

Atomic force microscopy (AFM) analysis

The surface topography of Ca-SA films at the micro-level was analyzed with an AFM (Dimension Icon, Bruker, Germany). The film was placed on a glass slide and all experiments were performed in air at ambient conditions. 3D topographic plots were obtained from five areas of film surface (30 × 30 μm^2), using the tapping mode at 1 Hz of scan rate. Roughness parameters (arithmetic average surface roughness (Ra) and root mean square roughness (Rq)) were also obtained from these images.

Mechanical properties measurement

The mechanical properties of film samples were determined in dry and wet states as alginate-based films are often used to manage exudative wounds. For the wet films' test, the crosslinked specimens were immersed in physiological saline solution (0.9 % w/v sodium chloride (NaCl)) for 30 s, and the excess of water removed with a filter paper. Tensile strength (TS) and percentage elongation at break (E %) were measured with a mechanical tensile tester (CMT6104-SANS, China), according to GB 13022-91. The samples were cut into strips with a width of 10 mm and had an effective length of 50 mm between the clamps at the beginning of the measurement. A crosshead speed of 5 mm/min was used. TS (MPa) was calculated by dividing the maximum load (N) required to break the film by the cross-sectional area (m^2), and %E was calculated by dividing the film elongation at rupture by its initial length and multiplying by 100. At least 10 replicates were run for each sample.

Statistical analysis

All statistical analyses were performed using a univariate analysis of variance. The data were presented as mean value ± SD.

Results and discussion

Influence of calcium concentration on gelation process

FTIR analysis

Figure 1 shows the FTIR spectra of SA films before and after crosslinking. The peaks at 3263, 1027, and 2925 cm^{-1} were assigned to stretching vibrations of –OH, –C–O–C– and –CH bonds, respectively [24, 25]. The strong peak at 1595 cm^{-1} and a somewhat weaker peak at 1408 cm^{-1} were attributed to the asymmetric and symmetric stretching vibration of the carboxylate group, respectively. Specially, these two peaks (1595 and 1408 cm^{-1}) were the most useful characteristic peaks to investigate the ion crosslinking (exchange) process [26–28]. It is evident that when the SA film was crosslinked with Ca^{2+}, the asymmetric –COO– vibrational peak shifted to a lower wavenumber (from 1595 to 1588/1590/1591 cm^{-1}) and the symmetric –COO– peak shifted to a higher wavenumber (from 1408 to 1415/1416 cm^{-1}). This could be due to the strong electrostatic interaction between Ca^{2+} and carboxylic groups of alginate. Furthermore, when the $CaCl_2$ concentration exceeded 0.75 % w/v, the wavenumbers of both the symmetric and asymmetric –COO– peaks did not change with the increase of $CaCl_2$ concentration. Considering that FTIR spectra recorded by ATR technique provide the specific structural information from the sample surface, we hypothesize that all potential Na^+ sites on film surface were exchanged with Ca^{2+} when the $CaCl_2$ concentration exceeded 0.75 % w/v.

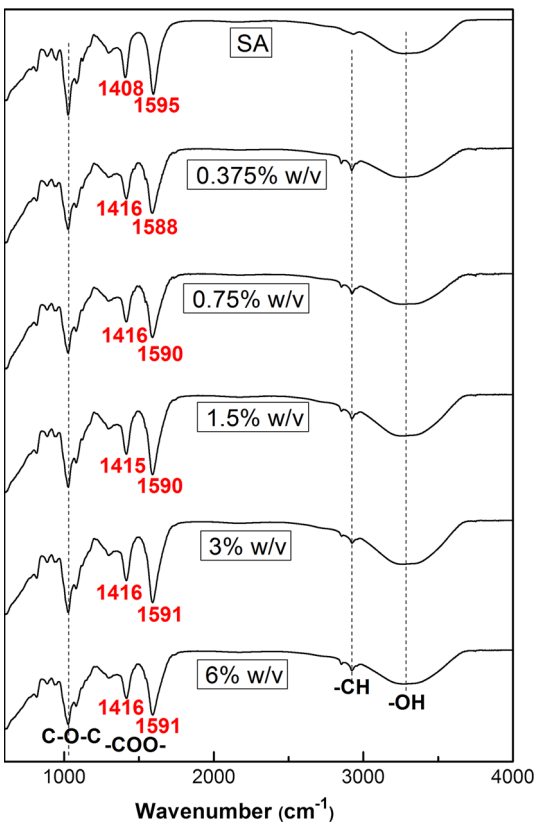

Figure 1 FTIR spectrums of SA and Ca-SA films crosslinked with various calcium chloride concentrations.

SEM and EDS analysis

The uniformity of Ca^{2+} crosslinking on the cross-sectional microstructure was analyzed using SEM and EDS mapping of sodium (Na, red) and calcium (Ca, green) (center and right side of Fig. 2). Previous reports indicated that high Ca^{2+} concentration caused instantaneous crosslinking, which resulted in heterogeneous structure with highly crosslinked surface and less crosslinking inside [29, 30]. However, simultaneous SEM and EDS results in Fig. 2 visually showed that the calcium element could distribute throughout the whole of the film matrix, regardless of the concentration of $CaCl_2$ in the crosslinking bath. This suggests that the $CaCl_2$ concentration did not influence the crosslinking uniformity of the whole films, which could be due to the fact that the increase in $CaCl_2$ concentration in crosslinking bath makes Ca^{2+} easy to diffuse into the film structure by thermodynamic driving forces, leading to the internal crosslinking reaction within the films. Furthermore, Ca^{2+} has a much smaller size than the large polymer molecule and can diffuse into the alginate matrix within the crosslinking time of 1 h in this work.

Visual appearance, swelling degree, and calcium content of alginate films

As shown in Fig. 3a, the wet Ca-SA films (immediately after crosslinking) crosslinked at a lower $CaCl_2$

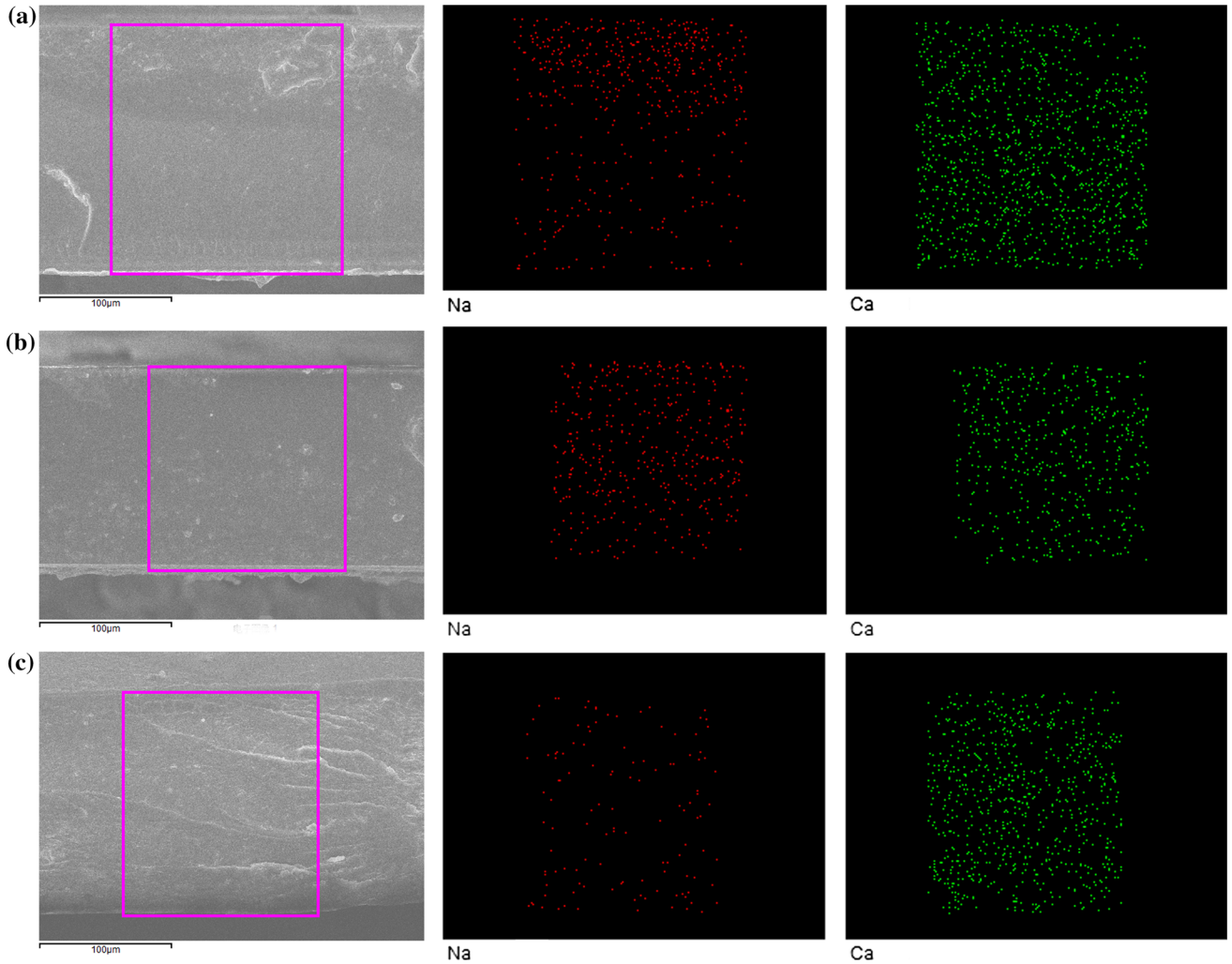

Figure 2 SEM and EDS spectrum (red for Na and green for Ca) of cross-section for Ca-SA films: **a** 0.375 % w/v, **b** 1.5 % w/v and **c** 6 % w/v. *Scale bar* 100 μm.

concentration (0.375 % w/v) displayed a slightly translucent and milk white-tinted appearance, which was a direct result of the high-swelling state of the film. Conversely, wet Ca-SA films became more and more optically clear with increasing $CaCl_2$ concentration, due to the drastically decreased swelling degree of films (as shown in Fig. 3a).

According to previous studies, the swelling degree (SD) of films can be used as a measure of the extent of crosslinking [30]. As shown in Fig. 3b (on the left), SD values of wet Ca-SA films decreased from 66.1 to 19.7 % when the $CaCl_2$ concentration increased from 0.375 to 6 % w/v. This result indicated that the whole crosslinking degree of films increased along with $CaCl_2$ concentration.

To further quantify the content of effective Ca^{2+} crosslinking sites, the calcium content within the dry Ca-SA films was determined by ICP-OES. Figure 3b (on the right) shows that the calcium content within films was first increased with the increasing of $CaCl_2$ concentration and then reached to a plateau when the $CaCl_2$ concentration exceeded 1.5 % w/v. These results further indicated that although all potential Na^+ sites on film surface were exchanged with Ca^{2+} when the $CaCl_2$ concentration exceeded 0.75 % w/v (FTIR spectra confirmed), the carboxylic-binding sites throughout the whole film matrix were not saturated unless the $CaCl_2$ concentration exceeded 1.5 % w/v. Similar saturation $CaCl_2$ concentration (1.4 % w/v) was reported by Cuadros et al. [18] for alginate fibers. Furthermore, it can be noted that the increase of calcium content within the films was not in synchrony with the increase of crosslinking degree (determined by SD), suggesting that aside from Ca^{2+}

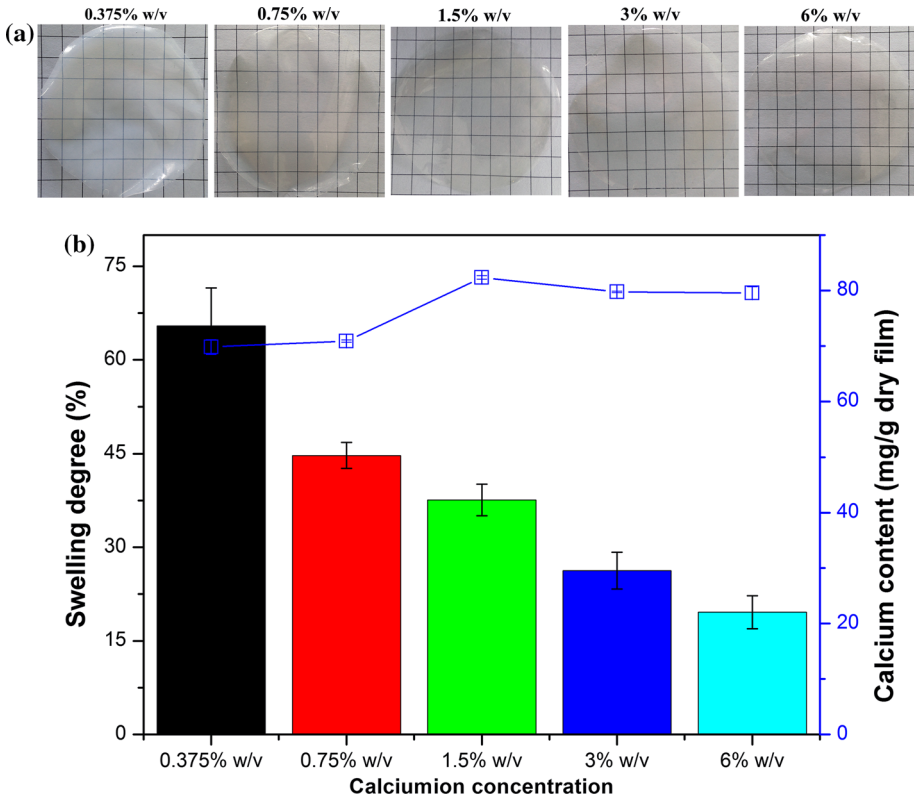

Figure 3 **a** Visual appearance of wet Ca-SA films after immersion in various crosslinking solutions. **b** Swelling degree (*left*) of wet Ca-SA films. **b** Calcium content (*right*) of dry Ca-SA films.

crosslinking sites, the films retained some other crosslinking sites, such as molecular chains entanglement.

Schematic evolution of gelation process with the increase of $CaCl_2$ concentration

To explain the effect of $CaCl_2$ concentration on the gelation process of calcium alginate films, proposed sequential events occurring within the alginate system along with the increase of $CaCl_2$ concentration are presented in Fig. 4.

It is known that the gel formation with Ca^{2+} and hydration of the SA occurred simultaneously when the SA films were soaked in crosslinking solution [30, 31]. And the SA molecules in the dry SA films expected to be substantially overlapped and entangled. At low $CaCl_2$ concentrations (<1.5 % w/v), it is likely that there would be insufficient ionic crosslinks to form a gel network, thus, the hydration of SA films would be dominant. As a result, the films were in a high-swelling state with less Ca^{2+}-binding sites and molecular chain entanglements. However, when the $CaCl_2$ concentration was slightly higher, the hydration of SA films would be partially counteracted by the Ca^{2+} crosslinking sites, which impeded the swelling of SA films. As $CaCl_2$ concentration further increased, the films crosslinked faster and the original molecular chain's entanglement of the SA films was almost retained. Based on the conceptual model, it is apparent from this work that the calcium concentration has a significant effect on the gelation process and can shape different crosslinking density and molecular entanglement characteristics within films.

Influence of calcium concentration on physical properties

Film thickness and visual appearance

For development of film used in pharmaceutics, film thickness is one of the parameters that could affect physicochemical properties of the films [28, 32]. Thickness of Ca-SA films in the wet state (immediately after crosslinking) and dry state is shown in Fig. 5a. The mean thickness of the dry SA film was about 0.076 mm. As shown in Fig. 5a, the wet Ca-SA films formed by predetermined $CaCl_2$ concentrations were significantly thicker than the dry SA film owing to the absorbed

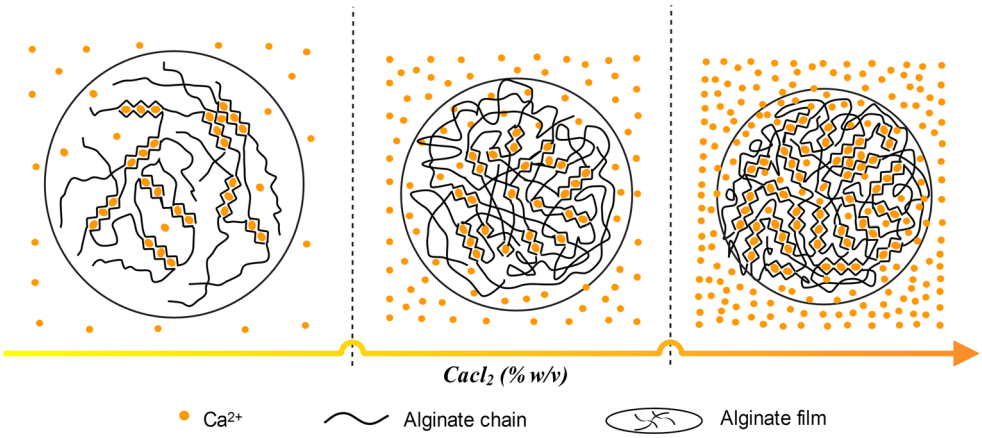

Figure 4 Schematic evolution of gelation process with the increase of calcium chloride concentration.

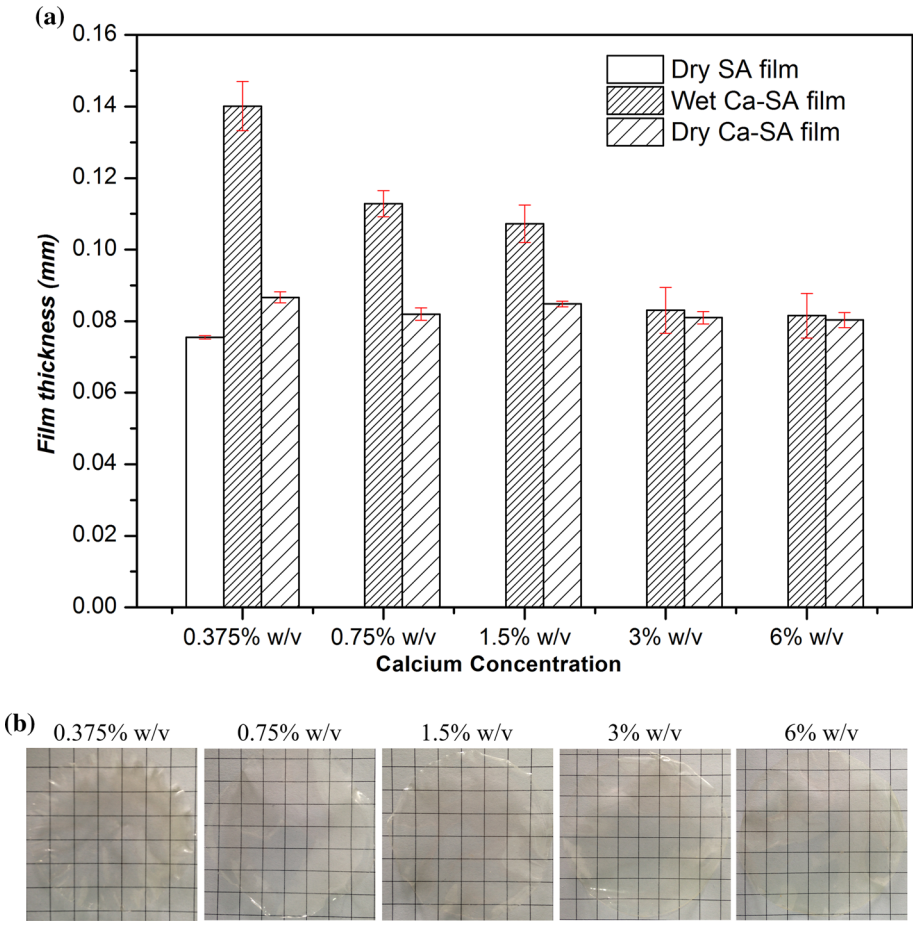

Figure 5 **a** Film thickness of SA (the dry state) and Ca-SA films (the wet and dry states) crosslinked with various calcium chloride concentrations. **b** Visual appearance of dry Ca-SA films.

water during crosslinking. However, when further increased the $CaCl_2$ concentration in crosslinking bath, wet Ca-SA films showed a marked decrease of thickness, which indicated that the higher $CaCl_2$ concentration crosslinking solution could inhibit the swelling (or hydration) of films. This correlated with the visual appearance and swelling degree results (as shown in Fig. 3). In addition, the thickness of dry Ca-SA films was slightly increased by crosslinking but not significantly influenced by the $CaCl_2$ concentration. The overall thickness variability in dry Ca-SA films with the increasing $CaCl_2$ concentration was similar and comparable to the previously studies involving SA films crosslinked in $CaCl_2$ water solution [21].

As shown in Fig. 5b, the visual appearance of dry Ca-SA films crosslinked at 0.75 % w/v $CaCl_2$ concentration was much more regular than that of films crosslinked at 0.375 % w/v $CaCl_2$ concentration. Furthermore, with the $CaCl_2$ concentration increased from 0.75 to 6 % w/v, the visual appearance of dry Ca-SA films did not show any significant difference.

Atomic force microscopy (AFM)

Figure 6a shows the images of AFM surface topography of dry Ca-SA films crosslinked in different $CaCl_2$ concentrations (0.375, 1.5 and 6 % w/v). As shown in Fig. 6a, the surface roughness decreased with the increase of $CaCl_2$ concentration. The roughness of the film surface was quantified using the roughness parameters Ra and Rq (Fig. 6b). The films crosslinked at 0.375 % $CaCl_2$ concentration have the highest Ra (29.5 nm) and Rq (37.1 nm) followed by films crosslinked at 1.5 % w/v (Ra = 25.2 nm, Rq = 33.9 nm) and 6 % w/v (Ra = 14.6 nm, Rq = 19.6 nm). These results are in line with the visual appearance (Fig. 5b) and further confirmed that crosslinking at higher $CaCl_2$ concentration seems to create more uniform films with reduced roughness. As reported in our previous work, surface roughness of dry Ca-SA films mainly depended on the swelling degree during crosslinking, as the highly swollen films resulted in polymer folding and formed heterogeneous surface during drying [23]. Therefore, the surface homogeneity of the films decreased with increasing $CaCl_2$ concentration could be due to the relatively lower swelling degree during crosslinking (the left of Fig. 3b).

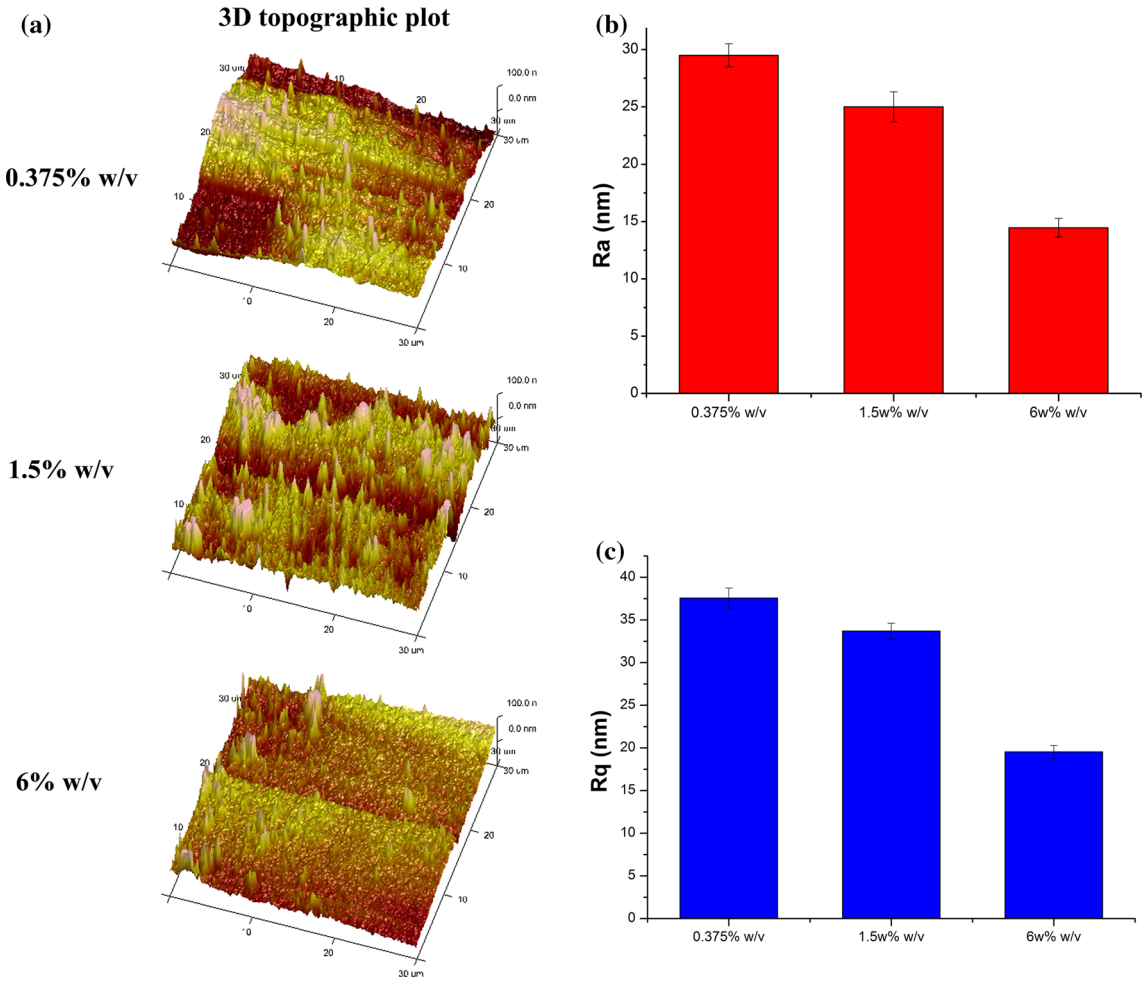

Figure 6 **a** AFM topographic images (30 μm × 30 μm) of dry Ca-SA films. **b** Arithmetic average surface roughness (Ra) of dry Ca-SA films. **c** Root mean square roughness (Rq) of dry Ca-SA films.

Swelling studies

As shown in Fig. 7, all samples displayed rapidly swelling first and then the swelling ratio (SR) reached equilibrium within a period of incubation. And sample from high $CaCl_2$ concentration resulted in lower SR at equilibrium and shorter the equilibration time of films. For example, films crosslinked at 0.375 % w/v $CaCl_2$ concentration exhibited the highest SR (0.55) at equilibrium and the equilibration was reached after about 30 min of immersion, while films crosslinked at 6 % w/v $CaCl_2$ concentration showed the lowest equilibrium SR (0.24) and the equilibration was reached after only 10 min of immersion. The different shaped crosslinking structure quality within Ca-SA films and the various osmotic strengths of coagulation bath can explain these swelling behaviors. On the one hand, a higher $CaCl_2$ concentration resulted in a higher crosslinking degree network and a denser structure, which caused a less swelling when it was soaked in distilled water. On the other hand, the osmotic strength of high $CaCl_2$ concentration coagulation bath may also 'suck' water out of the films. Conversely, a lower $CaCl_2$ concentration revealed less crosslinking and low osmotic strength, leading to significantly enhancement of water absorption. Furthermore, no significant weight loss was observed in all tested alginate after 24 h incubation (data not shown), which indicated that Ca^{2+} crosslinking improved the stability of alginate films.

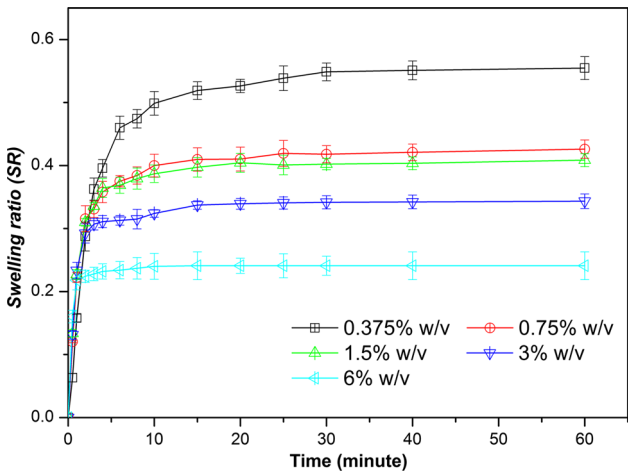

Figure 7 Swelling behavior of Ca-SA films immersed in distilled water at 25 °C.

Mechanical properties

The effects of $CaCl_2$ concentration used in crosslinking solution on the tensile strength (TS) and percentage elongation at break (E %) of Ca-SA films in both dry and wet states are illustrated in Fig. 8. In the

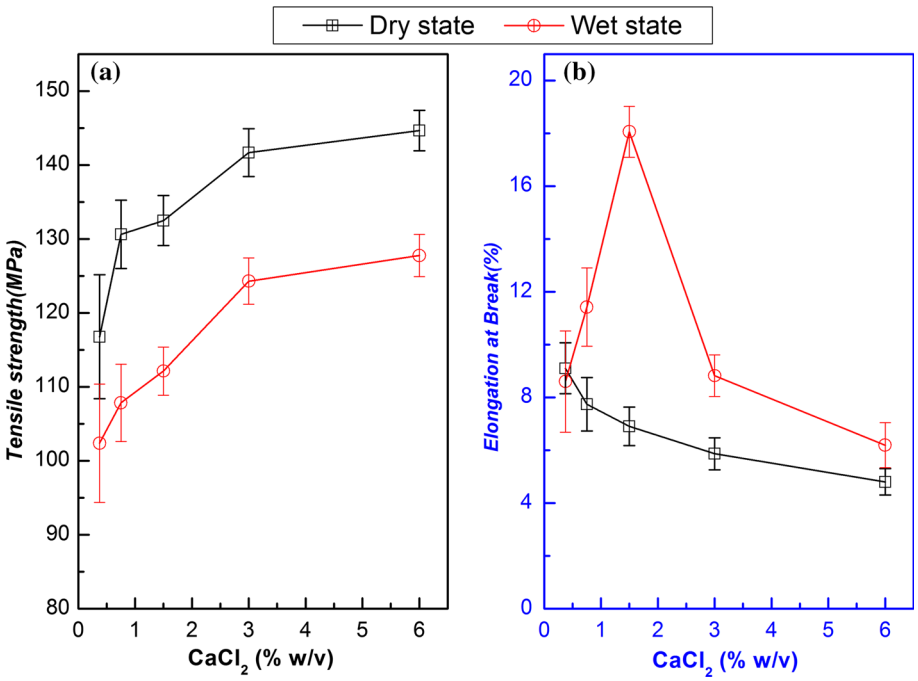

Figure 8 Mechanical properties of Ca-SA films crosslinked with various calcium chloride concentrations: Tensile strength (**a**) and elongation at break (**b**).

dry state, the TS value of Ca-SA films increased from 116.78 to 144.68 MPa with increasing the $CaCl_2$ concentration from 0.375 to 6 % w/v, whereas the E % value decreased from 9.11 to 4.81 %, which could be attributed to the increased crosslinking density within films.

Upon immersion of these Ca-SA films in 0.9 % w/v NaCl for 30 s, the TS values decreased and the E % values increased compared with those of dry Ca-SA films. This could be due to the plasticizing effect of the absorbed water molecules as well as the ion exchange between Ca^{2+} and Na^{+} during the immersion. Furthermore, TS values of films in the wet state continuously increased as the concentration of $CaCl_2$ increased. However, it was noted that as the $CaCl_2$ concentration increased, the E % reached its maximum value (18.06 %) and then decreased when the $CaCl_2$ concentration exceeded 1.5 %. This trend of E % values for wet Ca-SA films indicated again that in addition to Ca^{2+} crosslinking sites, the films might retain some molecular chains entanglement which can explain the ineffectiveness of $CaCl_2$ concentration on the variable E % values.

Conclusion

Alginate films crosslinked with different concentrations of $CaCl_2$ (0.375, 0.75, 1.5, 3, and 6 %, w/v) were successfully prepared by solution casting using the two-step crosslinking procedure. FTIR, swelling test, ICP-OES, and EDS analysis demonstrated the significant impact of $CaCl_2$ concentration on the gelation process of alginate films, due to the unique molecular entanglement and interactions between alginate and calcium ions at different $CaCl_2$ concentrations. The increase in $CaCl_2$ concentration in the crosslinking solution decreased the break elongation and swelling ability of alginate films, while improved the tensile strength and surface homogeneity. In addition, no significant changes in film thickness were detected with the increase of $CaCl_2$ concentration. As a compromise between film tensile strength and flexibility, performing effective absorption capability as well as the product appearance, the use of 1.5 % w/v $CaCl_2$ in the crosslinking step was recommended. The results of this work can be implemented to adjust the gelation process and obtain alginate films with proper physical properties, which could contribute to further biomedical applications. So, the effect of calcium concentration on the biomedical properties of alginate films should be emphasized in future research.

Acknowledgements

This work was supported by Weihai Science and Technology Development Plan Project (2013GNS028) and Shandong Province Postdoctoral Foundation (201101003). Experiments were conducted at the National Engineering Laboratory, WeGo Group Co., Ltd, Weihai, China.

References

[1] Dumitriu RP, Mitchell GR, Vasile C (2011) Multi-responsive hydrogels based on N-isopropylacrylamide and sodium alginate. Polym Int 60:222. doi:10.1002/pi.2929

[2] Ali G, Rihouey C, Vr Larreta-Garde, Le Cerf D, Picton L (2013) Molecular size characterization and kinetics studies on hydrolysis of pullulan by pullulanase in an entangled alginate medium. Biomacromolecules 14:2234. doi:10.1021/bm400371r

[3] Benykhlef S, Dulong V, Bengharez Z, Picton L, Guemra K, Le Cerf D (2012) Alginate grafted with poly (ε-caprolactone): effect of enzymatic degradation on physicochemical properties. Polym Int 61:1456. doi:10.1002/pi.4232

[4] Pankongadisak P, Ruktanonchai UR, Supaphol P, Suwantong O (2014) Preparation and characterization of silver nanoparticles-loaded calcium alginate beads embedded in gelatin scaffolds. AAPS PharmSciTech 15:1105. doi:10.1208/s12249-014-0140-9

[5] Pankongadisak P, Ruktanonchai UR, Supaphol P, Suwantong O (2015) Development of silver nanoparticles-loaded calcium alginate beads embedded in gelatin scaffolds for use as wound dressings. Polym Int 64:275. doi:10.1002/pi.4787

[6] Ichiura H, Konishi T, Morikawa M (2009) Alginate film prepared on polyethylene nonwoven sheet and its function for ellagic acid release in response to sodium ions. J Mater Sci 44:992. doi:10.1007/s10853-008-3220-y

[7] Petrusic S, Jovancic P, Lewandowski M et al (2013) Properties and drug release profile of poly(N-isopropylacrylamide) microgels functionalized with maleic anhydride and alginate. J Mater Sci 48:7935. doi:10.1007/s10853-013-7604-2

[8] Shi G, Che Y, Zhou Y, Bai X, Ni C (2015) Synthesis of polyglycolic acid grafting from sodium alginate through direct polycondensation and its application as drug carrier. J Mater Sci 50:7835. doi:10.1007/s10853-015-9363-8

[9] Ozhukil Kollath V, Chen Q, Mullens S et al (2015) Electrophoretic deposition of hydroxyapatite and hydroxyapatite–alginate on rapid prototyped 3D Ti6Al4 V scaffolds. J Mater Sci 51:2338. doi:10.1007/s10853-015-9543-6

[10] Venkatesan J, Bhatnagar I, Manivasagan P, Kang K-H, Kim S-K (2015) Alginate composites for bone tissue engineering: a review. Int J Biol Macromol 72:269. doi:10.1016/j.ijbiomac.2014.07.008

[11] Liu Y, Zhao J-C, Zhang C-J, Guo Y, Zhu P, Wang D-Y (2015) Effect of manganese and cobalt ions on flame retardancy and thermal degradation of bio-based alginate films. J Mater Sci 51:1052. doi:10.1007/s10853-015-9435-9

[12] Wang J, Wei J, Su S, Qiu J, Wang S (2015) Ion-linked double-network hydrogel with high toughness and stiffness. J Mater Sci 50:5458. doi:10.1007/s10853-015-9091-0

[13] Lee KY, Mooney DJ (2012) Alginate: properties and biomedical applications. Prog Polym Sci 37:106. doi:10.1016/j.progpolymsci.2011.06.003

[14] Morgan D (1997) Alginate dressings: part 1: historical aspects. J Tissue Viability 7:4. doi:10.1016/S0965-206X(97)80014-9

[15] Morgan D (1997) Alginate dressings: part 2: product guide. J Tissue Viability 7:9. doi:10.1016/S0965-206X(97)80015-0

[16] Qin Y (2008) Alginate fibres: an overview of the production processes and applications in wound management. Polym Int 57:171. doi:10.1002/pi.2296

[17] Qin Y (2005) Silver-containing alginate fibres and dressings. Int Wound J 2:172. doi:10.1111/j.1742-4801.2005.00101.x

[18] Cuadros TR, Skurtys O, Aguilera JM (2012) Mechanical properties of calcium alginate fibers produced with a microfluidic device. Carbohydr Polym 89:1198. doi:10.1016/j.carbpol.2012.03.094

[19] Akin Evingür G, Kaygusuz H, Bedia Erim F, Pekcan Ö (2014) Effect of calcium Ion concentration on small molecule desorption from alginate beads. J Macromol Sci Part B Phys 53:1157. doi:10.1080/00222348.2014.895625

[20] Xin Y, Bligh MW, Kinsela AS, Wang Y, Waite TD (2015) Calcium-mediated polysaccharide gel formation and breakage: impact on membrane foulant hydraulic properties. J Membr Sci 475:395. doi:10.1016/j.memsci.2014.10.033

[21] Crossingham YJ, Kerr PG, Kennedy RA (2014) Comparison of selected physico-chemical properties of calcium alginate films prepared by two different methods Int. J Pharm 473:259. doi:10.1016/j.ijpharm.2014.06.043

[22] Chan LW, Lee HY, Heng PW (2006) Mechanisms of external and internal gelation and their impact on the functions of alginate as a coat and delivery system. Carbohydr Polym 63:176. doi:10.1016/j.carbpol.2005.07.033

[23] Li J, He J, Huang Y, Li D, Chen X (2015) Improving surface and mechanical properties of alginate films by using ethanol as a co-solvent during external gelation. Carbohydr Polym 123:208. doi:10.1016/j.carbpol.2015.01.040

[24] Jana S, Samanta A, Nayak AK, Sen KK, Jana S (2015) Novel alginate hydrogel core–shell systems for combination delivery of ranitidine HCl and aceclofenac. Int J Biol Macromol 74:85. doi:10.1016/j.ijbiomac.2014.11.027

[25] Pongjanyakul T, Puttipipatkhachorn S (2007) Xanthan–alginate composite gel beads: molecular interaction and in vitro characterization. Int J Pharm 331:61. doi:10.1016/j.ijpharm.2006.09.011

[26] Cho AR, Chun YG, Kim BK, Park DJ (2014) Preparation of alginate–CaCl2 microspheres as resveratrol carriers. J Mater Sci 49:4612. doi:10.1007/s10853-014-8163-x

[27] Sartori C, Finch DS, Ralph B, Gilding K (1997) Determination of the cation content of alginate thin films by FTi. r. spectroscopy. Polymer 38:43. doi:10.1016/S0032-3861(96)00458-2

[28] Pongjanyakul T (2009) Alginate–magnesium aluminum silicate films: importance of alginate block structures. Int J Pharm 365:100. doi:10.1016/j.ijpharm.2008.08.025

[29] Pavlath A, Gossett C, Camirand W, Robertson G (1999) Ionomeric films of alginic acid. J Food Sci 64:61. doi:10.1111/j.1365-2621.1999.tb09861.x

[30] Rhim J-W (2004) Physical and mechanical properties of water resistant sodium alginate films. LWT Food Sci Technol 37:323. doi:10.1016/j.lwt.2003.09.008

[31] Goh CH, Heng PWS, Chan LW (2012) Cross-linker and non-gelling Na + effects on multi-functional alginate dressings. Carbohydr Polym 87:1796. doi:10.1016/j.carbpol.2011.09.097

[32] Khuathan N, Pongjanyakul T (2014) Modification of quaternary polymethacrylate films using sodium alginate: film characterization and drug permeability. Int J Pharm 460:63. doi:10.1016/j.ijpharm.2013.10.050